Search for Sulfur (H_2S) on Jupiter at Millimeter Wavelengths

Joanna Joiner, *Member, IEEE,* Paul G. Steffes, *Senior Member, IEEE,* and Keith S. Noll

***Abstract*—We have observed Jupiter at two wavelengths near 1.4 mm in an attempt to detect gaseous hydrogen sulfide (H_2S) or place new upper limits on its abundance in Jupiter's atmosphere. Although we were not successful in detecting H_2S, we report the first brightness temperature observations of Jupiter at 1.4 mm with a spectral resolution of approximately 1 GHz using Mars as the calibration standard. We also discuss the methodology and results of a laboratory experiment in which we measured H_2S absorption at 1.4 mm in a simulated Jovian atmosphere (predominantly H_2 and He). We apply the results of our laboratory measurements to a radiative transfer model which we use to interpret our observations of Jupiter.**

I. Introduction

Sulfur is the tenth most abundant element in the solar system [1]. Although sulfur has been detected on Jupiter's volcanic moon Io, it remains mysteriously absent from the list of elements detected in the massive atmospheres of the gaseous giant or Jovian planets (Jupiter, Saturn, Uranus, and Neptune). Ground-based observation with radio telescopes provides one of the few means capable of probing beneath the dense cloud layers of the Jovian planets where sulfur in the form of gaseous hydrogen sulfide (H_2S) may be found. Jupiter presents the best target for the H_2S search due to its cloud structure. Determination of the sulfur abundance in the giant planet atmospheres would provide valuable information needed to develop and refine models of the origin and evolution of the planets and solar system. The search for sulfur is also of interest relative to the long-standing problem of the unknown composition of colored cloud materials in Jupiter. Because ammonium polysulfides and other sulfur compounds are leading candidates for this material [26], detection of any sulfur containing molecule would be of great value.

Manuscript received May 14, 1991; revised December 26, 1991. This work was supported by the Planetary Atmospheres Program of the Solar System Exploration Division (Office of Space Science and Applications) of the National Aeronautics and Space Administration under Grant NAGW-533 and by the Georgia Tech Space Grant Consortium.

J. Joiner was with the School of Electrical Engineering, Georgia Institute of Technology, Atlanta, GA 30332-0250. She is currently with USRA/NASA-Goddard Space Flight Center, Code 910.4, Greenbelt, MD 20771.

P. G. Steffes is with the School of Electrical Engineering, Georgia Institute of Technology, Atlanta, GA 30332-0250.

K. S. Noll was with NASA/Marshall Space Flight Center, Huntsville, AL 35812. He is currently with the Space Telescope Science Institute, 3700 San Martin Drive, Baltimore, MD 21218.

IEEE Log Number 9107706.

Both theory and previous observation suggest that sulfur is depleted in and above Jupiter's troposphere. Thermo-chemical equilibrium models predict that H_2S combines with ammonia (NH_3) to form an ammonium hydrosulfide (NH_4SH) ice cloud near the 2 bar pressure level on Jupiter (see, [2] or [11]). If the H_2S abundance is less than the NH_3 abundance at sub-cloud altitudes in Jupiter's atmosphere, the reaction

$$NH_3(\text{gas}) + H_2S(\text{gas}) \overset{K}{\rightleftharpoons} NH_4SH(\text{solid}) \quad (1)$$

should rapidly deplete H_2S above the cloud. Any H_2S which escaped destruction in the reaction to form NH_4SH should be destroyed by photolysis near 1 bar [3]. Infrared observations of Jupiter at 2.7 μm by Larson *et al.* [13] provide a strict upper limit on the H_2S abundance at pressures between 0.7 and 1.2 bar. This limit confirms that H_2S is indeed depleted in Jupiter's upper troposphere.

Millimeter-wave observations probe altitudes in Jupiter's atmosphere at and below the altitude of the putative NH_4SH cloud, where gaseous H_2S may exist. Bezard *et al.* [3] suggested that H_2S lines might affect Jupiter's millimeter wavelength emission. There are three strong millimeter rotational H_2S lines centered at 168.8, 216.7, and 300.5 GHz (1.78, 1.38, and 1.00 mm). The best spectral region to search for H_2S is near the 216.7 GHz H_2S line. At this frequency, the atmospheres of both Jupiter and the earth are relatively transparent. In Jupiter's atmosphere, NH_3 opacity obscures the potential effects of H_2S lines at frequencies $\geq$300 GHz (wavelengths $\leq$1 mm). Interference from the 183 GHz water vapor line in the earth's atmosphere would complicate an observation of the 168.8 GHz H_2S line.

Detecting the 216.7 GHz (1.4 mm) H_2S line with existing instrumentation is difficult. The line is pressure-broadened by hydrogen (H_2) and helium (He) (the major constituents in Jupiter's atmosphere), spreading its total width over 30–40 GHz ($\Delta\nu/\nu \sim 10^{-1}$). Most of the existing observations of Jupiter at millimeter wavelengths have been made with broad-band filters which have passbands of approximately 70 GHz. These filters average the emission detected in the passband, effectively smearing any smaller scale spectral features such as pressure-broadened H_2S lines. Other receivers used in millimeter and submillimeter astronomy are designed to detect narrow emission lines ($\Delta\nu/\nu \sim 10^{-4}$) in the interstellar medium. These receivers typically have passbands less than 1 GHz which would be too narrow to detect pressure-broadened H_2S lines.

Our approach was to observe Jupiter's emission at two or more frequencies with a high-resolution receiver. Any significant difference in emission at the different frequencies can be attributed to H_2S absorption. We also used Mars as the primary calibrator to derive reliable brightness temperatures of Jupiter near 1.4 mm.

In order to accurately model the potential effects of H_2S opacity on the radio emission from the giant planets and interpret observational results correctly, the pressure-broadening of hydrogen sulfide lines by hydrogen and helium must be measured. This paper describes a laboratory experiment in which we measured the pressure-broadened linewidth of hydrogen sulfide in a simulated Jovian atmosphere at 1.4 mm. This is the same wavelength at which we observed Jupiter. This measurement represents the first time an H_2S pressure-broadened linewidth has been measured in a predominantly hydrogen/helium atmosphere. We discuss the results of this laboratory measurement and their application to the Jupiter observation.

II. Dual Wavelength Observation of Jupiter at 1.4 mm

A. Instrumentation and Procedure

The primary objective of our observation was to detect the potential dip in Jupiter's spectrum resulting from H_2S absorption. We used the total bandwidth of the spectrometer as a bandpass filter or photometer at two frequencies. We first observed Jupiter near the H_2S line center where the potential H_2S absorption is at a maximum. We then observed Jupiter at a frequency off the line center where the H_2S opacity is small (i.e., the continuum). Fig. 1 shows the potential effect of H_2S on Jupiter's spectrum at 216 GHz (1.4 mm). The dotted and solid lines are synthetic Jovian spectra with and without H_2S absorption, respectively. We also show the observed double sideband frequencies. We observed Jupiter and Mars with the LO centered at 215.3 GHz and 229.6 GHz. We were unable to tune the receiver to the low frequency tail of the H_2S line due to instrumental problems. In order to infer H_2S absorption, we need only measure a differential emission between two or more wavelengths. Lellouch *et al.* [12] used a similar approach to search for PH_3 and HCN spectral features on Jupiter. A secondary objective of our observation was to obtain a reliable brightness temperature of Jupiter at this wavelength. This requires a precise estimate of the brightness temperature of Mars, which was used as the primary calibrator.

The observations were made with the 10.4 m Caltech Submillimeter Observatory (CSO)[1] at Mauna Kea, Hawaii. The double sideband (DSB) receiver has a band separation of 2.8 GHz (IF-band 1150–1650 MHz). The Acousto-Optic Spectrometer (AOS) has a total bandwidth of 500 MHz and 1024 channels. The receiver temperatures (DSB) measured at 215 and 230 GHz were 220K and 240K, respectively.

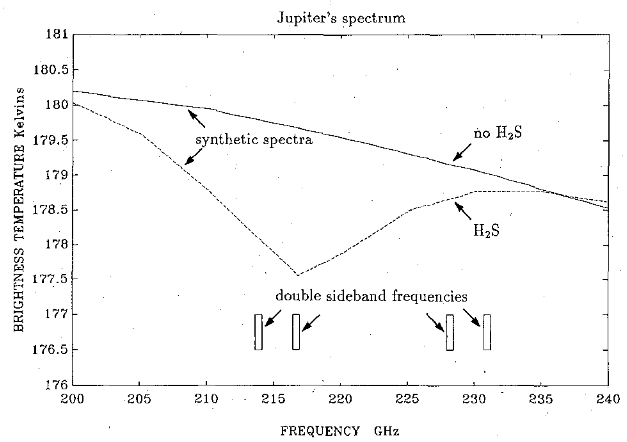

Fig. 1. Effect of H_2S absorption near 220 GHz and frequencies at which we observed Jupiter with the double sideband (DSB) CSO receiver. Dashed line: spectrum with H_2S absorption, solid line: spectrum without H_2S absorption.

The receiver required careful tuning at each frequency of observation. Tuning the receiver involved the manual adjustment of several back-shorts and attenuators in order to optimize the receiver temperature. Because the two frequencies we chose were separated by approximately 15 GHz, it was not possible to use a single local (Gunn) oscillator (LO). Changing oscillators increased the time required to tune the receiver. We required between 45 minutes and 2 hours to achieve adequate receiver temperatures.

Chopping was accomplished by position switching or alternately pointing the telescope ON the source (planet) and then at a position in the sky OFF the source 5 feet in either the + or − azimuth direction. The telescope remained both ON the source and OFF the source for a duration of 10 seconds. One scan of the source is defined as 4 ON/OFF cycles resulting in a total integration time of 80 seconds.

Accurate telescope pointing was accomplished by constructing a five point map of the planet. An on-line program used a Gaussian fit to position the planet in the center of the telescope beam. The pointing remained accurate to better than 4″ (or ~10%) between repositioning which typically took place after every other scan.

We observed both Jupiter and Mars on (UT) November 25, 1990 with the LO centered at 215.3 GHz so that the H_2S line (216.7 GHz) was centered in the upper sideband. We observed Mars first, then Jupiter, followed by Mars again, checking for variation in the observed temperature of Mars. We observed no variation in the temperature of Mars on that night. We used the same procedure to observe the two planets on (UT) 26 November, 1990 at a frequency 229.6 GHz. This frequency was chosen so that the 230.5 GHz CO line, which has been observed in the Martian spectrum, would be between the upper and lower sidebands. Therefore, it would not interfere with our con-

[1]The CSO is operated by the California Institute of Technology under funding from the National Science Foundation, Contract #AST-88-15132.

tinuum observation of Mars. Some variation occurred in the observed antenna temperature of Mars at this frequency prior to and following the observation of Jupiter. This variation results in a large uncertainty in the observed temperature of Mars and thus a large uncertainty in the Mars/Jupiter ratio at this frequency. The receiver was then retuned to a center frequency of 215.3 GHz to repeat the November 25 observation. We observed Mars followed by Jupiter. We were unable to observe Mars a second time due to the low elevation of Mars and deteriorating weather conditions.

B. Calibration

The computer automatically executed a chopper wheel calibration scan before scanning the planet. This calibration procedure removed the effects of the earth's atmospheric opacity [16]. Because our source and calibrator have finite and different angular sizes, additional calibration steps were required.

For a source (planet) whose size is comparable to the size of the antenna beam, the product of the cold spillover efficiency, β, and the source coupling efficiency, γ, can be computed from

$$\beta\gamma\,(\text{Main Beam}) = \left[\frac{T_A^*(\text{Planet})}{2T_{\text{Planet}}}\right] \cdot \left[1 - \exp\left[-\left(\frac{D}{\Theta}\right)^2 \ln 2\right]\right]^{-1}, \quad (2)$$

[16] where D is the angle subtended by the planet, Θ is the telescope beamwidth (FWHM), T_{Planet} is the actual or estimated brightness temperature of the planet, and T_A^* is the observed antenna temperature (automatically corrected by the computer for atmospheric effects and telescope losses). Mars is an ideal calibrator. It is bright, compact, and its tenuous atmosphere gives rise to a relatively flat millimeter-wave spectrum (with the exception of a few narrow lines such as the CO line mentioned above). The Martian brightness temperature can be predicted with good accuracy. Using the observed T_A^* (Mars) and assuming T_{Mars} based on radiative transfer models and previous observations, $\beta\gamma$ can be computed from (2). Then, $\beta\gamma$ is used to compute Jupiter's brightness (T_{Jupiter}) from the observed antenna temperature T_A^* (Jupiter).

In (2), the second term represents a correction for the partial filling of the antenna beam [21]. For Jupiter, we use an equatorial radius at the 1 bar level of 71495 km and an ellipticity of 0.065. This value is based on the Voyager radio occultation experiment [9]. A value of 3397 km was assumed for the Mars equatorial radius with an ellipticity of 0.0006. These are the same radii as those used by Griffin *et al.* [14]. During the epoch of our observation, the angle subtended by Mars was approximately 18″. Jupiter's size was approximately 40.6 inches × 38″.

In order to infer the antenna beamwidth (Θ), we obtained a 230 GHz map of Jupiter from Schinckel (private communication, 1991). The beam map was deconvolved with a model of Jupiter's expected emission which takes into account the effects of its oblate shape and limb darkening. The resulting antenna pattern was Gaussian with a FWHM of 45.9 inches at 230 GHz. Assuming the antenna illumination efficiency to be constant over the 215.3 to 230 GHz range, the FWHM at 215.3 GHz is 49.0″.

We estimated the brightness temperatures of Mars to be 211.9 and 212.6 K at 216 and 230 GHz, respectively. The estimates are based on a radiative transfer model developed by *Rudy et al.* [18], [19]. Rudy's model accounts for both seasonal and longitudinal variation. The model predicts a longitudinal variation in the Martian brightness temperature of less than 1K or 0.5% during the epoch of our observation. Since Rudy's model is extrapolated from observations at 2 and 6 cm, we have used an additional check. Ulich [22] has developed the only model for predicting the Martian brightness temperature based on millimeter wavelength observation using absolute calibration. Ulich's model is limited in that it is based on observations at a single frequency (86 GHz or 3.5 mm) and only takes into account seasonal variation. Ulich's empirical expression predicts a temperature of 208.1 ± 1.5 K at 86 GHz. Rudy's model predicts the brightness temperatures over one rotation of Mars to vary between 197 and 203K at 86 GHz. The two models agree to within about 5%.

Previous observers have stated the uncertainty in the Martian brightness temperature to be ±10% or approximately ±20 K [9]. Muhleman and Berge [15] have recently reported an uncertainty in the Martian brightness temperature of ±3% or ±6 K. Our estimation of the Martian brightness temperature using Rudy's model is similar to that of Muhleman and Berge [15]. We used an effective dielectric constant of 2.5 and a (power) absorption length of 15 wavelengths in Rudy's model to compute the Martian brightness temperature for the epoch of our observation (L_s = 338°.9). Although Rudy (private communication, 1991) estimates the uncertainty in his model to be somewhat better than 10%, we will assume the uncertainty in the Martian brightness temperature to be ±10%. It should be noted that this is the same uncertainty used by previous observers [9] and it is a conservative estimate compared with that of Muhleman and Berge [15].

Ideally, the observations of Jupiter should be made when the calibrator (Mars) is close to the source (Jupiter) in the sky. In that case, the effects of any temporal or spatial variation in the earth's atmospheric opacity would be limited. However, good observations of Jupiter relative to Mars can still be made even if the planets are not ideally positioned. During our observation, Jupiter reached zenith approximately 5 hours after Mars. We were careful to observe Jupiter and Mars at times when the atmospheric opacity was observed to be stable and both planets were at similar elevations. The amount of observing time satisfying these conditions was limited.

The atmospheric opacity was monitored by accessing data from the NRAO/SAO 225 GHz Atmospheric Re-

TABLE I
OBSERVED ANTENNA TEMPERATURES

Freq. (GHz)	Date (UT)	Source	$T_A^* \pm 1\sigma$ (K)	$\beta\gamma$	Comments
215.31	11/25/90	Mars	59.7 ± 0.4	0.825	All scans (2 sets)
215.31	11/25/90	Jupiter	154.9 ± 6.7		All scans (1 set)
			161.6 ± 1.2		scans starting ON source only
			148.2 ± 0.9		scans starting OFF source only
215.31	11/25/90	Mars	51.4 ± 0.6	0.713	All scans (1 set)
215.31	11/26/90	Jupiter	141.8 ± 6.4		All scans (2 sets)
			147.5 ± 1.2		scans starting ON source only
			134.7 ± 2.5		scans starting OFF source only
229.60	11/26/90	Mars	60.5 ± 4.4	0.743	All scans (2 sets)
			54.8 ± 0.4	0.673	Low's only
			63.6 ± 0.7	0.782	High's only
229.60	11/26/90	Jupiter	154.5 ± 12.9		All scans (1 set)
			169.2 ± 1.5		scans starting ON source only
			143.4 ± 1.3		scans starting OFF source only

ceiver located next to the CSO. This instrument is a radiometer which measures the earth's atmospheric emission at several elevations in order to determine the atmospheric transmission and corresponding zenith optical depth. The zenith optical depth, τ_z, was stable at 0.05 on 25 November for approximately three hours. On November 26, τ_z was higher but relatively stable at 0.2 for approximately four hours. We were unable to observe on the first scheduled night of observation (November 24) due to poor weather conditions.

C. Results

Using the data analysis package CLASS, we fit a zero order baseline to the observed spectrum of each scan. We averaged the antenna temperature (T_A^*) over the 1024 AOS channels to reflect a mean and RMS deviation for each scan. The overall observational uncertainty was dominated by scatter in the means of individual scans, not the baseline ripple observed in a single scan. As expected, we were limited by sky noise and systematic errors, not the receiver sensitivity. The averaged observed antenna temperatures, T_A^*, are listed in Table I. We also list our computed values of $\beta\gamma$. The expected value of $\beta\gamma$ at 230 GHz was approximately 0.72. We note that our observed values of $\beta\gamma$ varied from night to night by as much as 10%.

We also note systematic variations in both the Jupiter and Mars scans. The Jupiter scans which began with the telescope ON the planet resulted in consistently higher antenna temperatures than scans which began with the telescope OFF the planet (on the sky). We believe that the computer-controlled attenuators were not set to adequate levels during the scans which began OFF the source. This would cause compression of the amplifiers which would result in lower measured antenna temperatures. Compression of the amplifiers was observed independently by Schinckel (private communication, 1991). Therefore, we believe that only the scans which started ON Jupiter are reliable and include only these scans in our calculation of Jupiter's brightness temperatures.

We list the data used to derive Jupiter's brightness temperature at 215 and 230 GHz in Table II. The uncertainty in Jupiter's brightness temperatures (T_{Jupiter}) for individual nights is the root sum square of the observed uncertainties in T_A^* for Mars and Jupiter (note: This does not include the additional ±10% uncertainty in the estimated Martian brightness temperature).

We report our observed brightness temperatures of Jupiter along with those of previous observations near 1.4 mm in Table III. The first uncertainty represents the 1σ statistical uncertainty in the Mars/Jupiter ratio, appropriate for searching for possible spectral features. The second uncertainty includes the additional 10% uncertainty in the assumed Martian brightness temperature required for calibrated brightness temperature measurements. Our observed brightness temperatures are in relatively good agreement with previous observations at wavelengths near 1.4 mm [17], [6], [23], [9]. It should be noted that all of the previous observations were made with broad-band filters, and only Courtin *et al.* [6] and Griffin *et al.* [9] used Mars as the calibrator. Rather *et al.* [17] and Ulich *et al.* [23] assigned brightness temperatures of 150K and 165K, respectively, to Jupiter based on their observations of several planets and previously observed planetary brightness temperatures at longer and shorter wavelengths.

Finally, we chose to utilize the spectral information available in the 1024 AOS channels to obtain additional calibration information and to check for the unlikely presence of a narrow line core emission from H_2S in Jupiter's stratosphere. We observed line emission from the core of the Orion molecular cloud on both nights at 215.3 GHz in addition to the two planets. The hydrogen sulfide line emission from Orion at 216.7 GHz (centered in the upper sideband) was clearly visible after one scan. If an H_2S emission core was present in the Jupiter scans, it would also be centered in the upper sideband.

We observed no H_2S emission core when all of the Jupiter scans were averaged. This results in a stratospheric H_2S mixing ratio upper limit of approximately 1×10^{-6}. This limit is not as tight as previous upper limits of Ju-

TABLE II
OBSERVATIONAL DATA USED TO COMPUTE JUPITER'S BRIGHTNESS TEMPERATURE

Freq. (GHz)	Date (UT)	$T_A^* \pm 1\sigma$ Mars	$T_A^* \pm 1\sigma$ Jupiter	T_{Mars} Estimated	T_{Jupiter} Observed
215.31	11/25/90	59.7 ± 0.4	161.6 ± 1.2	211.9	166.3 ± 1.7
215.31	11/26/90	51.4 ± 0.6	147.5 ± 1.2	211.9	175.0 ± 2.5
229.60	11/26/90	60.5 ± 4.4	169.2 ± 1.5	212.6	178.1 ± 13.0
229.60	11/26/90	54.8 ± 0.4	169.2 ± 1.5	212.6	196.7 ± 2.3
229.60	11/26/90	63.6 ± 0.7	169.2 ± 1.5	212.6	169.4 ± 2.4

TABLE III
OBSERVED BRIGHTNESS TEMPERATURES OF JUPITER NEAR 1.4 mm

Wavelength (mm)	Freq. (GHz)	T_B^a (K)	Calibrator	$\Delta\nu$ (GHz)	Reference
1.30	231	175.0 ± 2.5(18)	Mars	3.2	This work
1.32	227	170.9 ± 3.9(18)	Mars	70	Griffin *et al.* (1986)
1.32	227	165 ± 8(18)	planets	39	Ulich *et al.* (1984)
1.39	216	178.11 ± 13.0(22)	Mars	3.2	This work
1.40	214	148 ± 16(22)[b]	planets	275	Rather *et al.* (1975)
1.40	214	168 ± 11(20)[c]	Mars	210	Courtin *et al.* (1977)

[a] First uncertainty is 1σ observational uncertainty, the second uncertainty includes an additional 10% for absolute calibration.
[b] Brightness temperatures as corrected in Berge and Gulkis (1976).
[c] Recalculated using beam correction factor in Ulich (1980).

piter's stratospheric H_2S abundance (as low as 1×10^{-9}) based on observations at several wavelengths from the infrared to uv (summarized by Larson *et al.*, [13]).

The line intensities in the Orion spectra also provide a secondary calibration source. We obtained good agreement between our spectra of Orion taken on 26 November and those of Sutton *et al.* [20]. However, the line intensities of the spectra taken on November 25 are significantly higher than those of Sutton *et al.* [20]. This could be due to a sideband ratio $\neq 1$. This might also explain the high value of $\beta\gamma$ observed on November 25. Therefore, we believe the November 26 observation to be more reliable than the November 25 observation.

III. MEASUREMENT OF (H_2S) OPACITY AT 1.4 mm

One of the outstanding problems in millimeter spectroscopy of planets has been and continues to be the lack of adequate laboratory measurements of lineshapes and linewidths of gases at relevant pressures and temperatures and with appropriate broadening agents. Since H_2S absorption has never been measured under Jovian conditions (i.e., predominantly hydrogen atmosphere), we have configured a system capable of making such measurements. We use the results to intepret our Jupiter observations.

A. *Laboratory Configuration and Procedure*

A block diagram of the laboratory configuration used to measure H_2S absorption is shown in Fig. 2. The *G*-band CW signal (~218 GHz) was generated by doubling a W-band (~109 GHz) klystron tube source. The klystron power supply provided 1 KHz modulation by varying the klystron reflector voltage. The resulting frequency variation was less than 0.5%. Since the pressure-broadened H_2S linewidth was several GHz, absolute frequency stability was not necessary. The modulation signal incident on the frequency doubler was monitored with an oscilloscope. The klystron signal was sampled with a 20-dB coupler and downconverted to an IF of approximately 800 MHz using a harmonic mixer. A microwave source phase-locked to a microwave frequency counter provided the mixer's LO. The IF frequency and stability was monitored with a high-resolution spectrum analyzer. The exact klystron frequency was computed from the precise measurement of the IF and LO frequencies using the spectrum analyzer and frequency counter.

The *G*-band signal was transmitted through a 71 cm glass cell and received using high-gain horn antennas. We aligned the antennas with a helium-neon laser as illustrated in Fig. 3. A *G*-band square law detector converted the received millimeterwave signal to a voltage which was measured with a lock-in amplifier. A 5-cm piece of WR-5 waveguide (f_c = 168 GHz) acted as a high-pass filter to prevent any leakage of the fundamental or first harmonic (~109 GHz). We used a high-pass filter (f_c = 300 GHz) to measure the amplitude of the third harmonic (~327 GHz). The power from the third harmonic was more than 30 dB down from the second harmonic. Therefore, the detector was measuring power from mostly the desired second harmonic (~218 GHz).

A relatively large H_2S mixing ratio was needed to measure absorption in the cell. We used a pre-mixed, constituent analyzed gas mixture (Matheson) in all experiments. This mixture consisted of 78.79% H_2, 9.28% He

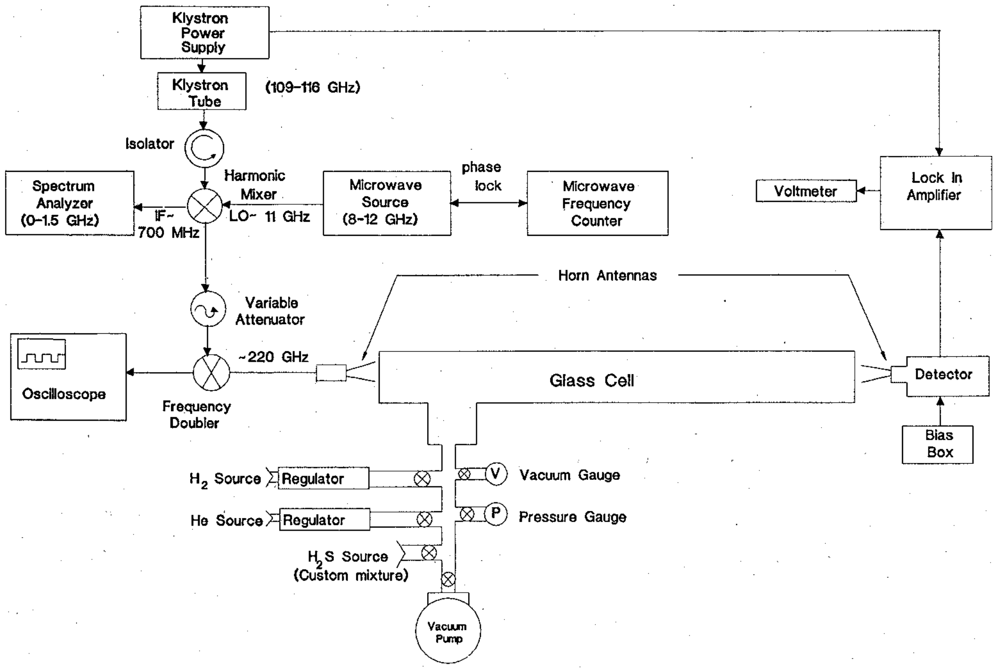

Fig. 2. Block diagram of the laboratory configuration used to measure millimeterwave H_2S absorption in a simulated Jovian atmosphere.

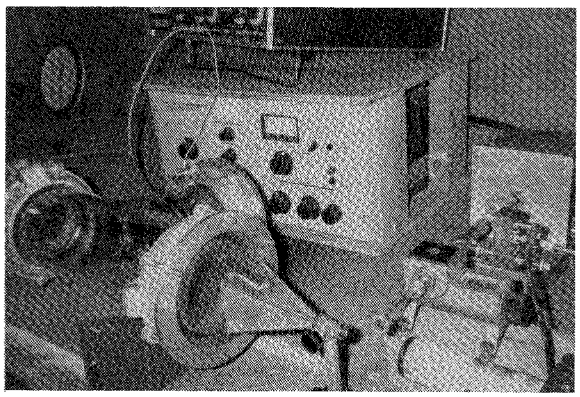

Fig. 3. Laser alignment of the laboratory instrumentation.

and 11.93% H_2S. The uncertainty in the mixture was $\pm 2\%$ of the stated component mixing ratio. The experiments took place at ambient temperature (296K) and at a total pressure of 2 atm.

We first measured the power or voltage on the detector with the H_2-He-H_2S gas mixture in the cell. We then measured the power with a 90% H_2-10% He gas mixture in the cell. Reflections occur at the cell boundaries due to the different dielectric constants of the air outside the cell, gas mixture in the cell, and lenses at the cell boundary. The indices of refraction for the two gas mixtures with and without H_2S at STP are approximately 1.000183 and 1.000122, respectively. Reflections occurring at the cell boundaries should be similar for both gas mixtures. In a less rigorous check, we observed no difference in reflection between the H_2/He mixture and a mixture of 70% H_2 and 30% air which has exactly the same index of refraction as the H_2S mixture. The absorption due to the H_2-He mixture was negligible. The attenuation due to the H_2S mixture is computed from the ratio of the voltage measured with the H_2-He-H_2S gas mixture in the cell to the that measured with the H_2-He mixture. This approach ensures that the drop in signal level is due only to absorption and not to changes in reflection at the cell interfaces.

The main source of uncertainty in this experiment was power drift in the klystron source. Power and frequency drifts occurred as the klystron temperature varied. We found that the klystron output power exhibited a sinusoidal drift, even though it was mounted on a large heat sink. The drift period was substantially longer than the time required to make an individual measurement. By obtaining several measurements, we characterized the drift and minimized this uncertainty. The overall uncertainty in klystron power was approximately $\pm 7\%$. Other instrumental uncertainties include uncertainty in the measurement of temperature ($\pm 1\%$), total pressure ($\pm 7\%$), and the above stated uncertainty in the H_2S mixing ratio. The total uncertainty in the measured absorption coefficient is the root sum square of the individual uncertainties.

B. Experimental Results

The pressure-broadened H_2S linewidth in an H_2-He atmosphere ($\Delta\nu$) is approximated by

$$\Delta\nu = \left(\frac{T}{T_o}\right)^{-n} [\Delta\nu_{H_2} P_{H_2} + \Delta\nu_{He} P_{He} + \Delta\nu_{H_2S} P_{H_2S}], \quad (3)$$

where $\Delta\nu_{H_2}$, $\Delta\nu_{He}$, $\Delta\nu_{H_2S}$ are the hydrogen, helium, and self-broadened H_2S linewidths, P_{H_2}, P_{He}, and P_{H_2S} are the partial pressures of hydrogen, helium, and hydrogen sulfide, T is temperature, and T_o is a normalizing temperature (296K). The temperature scaling exponent, n, has not

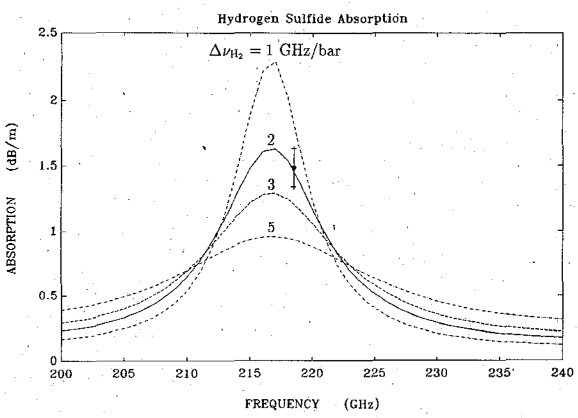

Fig. 4. Measured absorption and theoretically derived absorption in a 78.79% H_2-9.28% He-11.93% H_2S mixture at 2 bar and 296K using the Van Vleck-Weisskopf lineshape for several values of $\Delta\nu_{H_2}$.

been measured for H_2S. We assumed a value of $n = 0.67$ based on the measured nitrogen-broadened 183 GHz H_2O linewidth [25]. Because our measurement was conducted at room temperature, the assumed value of n did not affect our results. Moreover, the value of n does not significantly affect the linewidth calculation when temperatures are extrapolated to lower temperatures occurring in Jupiter's atmosphere. For example, changing the value of n to 0.3 (which we estimate to be a lower limit) at 200K (the temperature of Jupiter's atmosphere near 2 bar) results in a linewidth difference of less than 20%.

Helminger and De Lucia [10] measured the 217 GHz self-broadened H_2S linewidth ($J'_{K'_{-1}K'_{+1}} - J_{K_{-1}K_{+1}} = 2_{0,2} - 2_{1,1}$) and report a value of $\Delta\nu_{H_2S} = 9.10$ MHz/Torr (6.92 GHz/bar). Willey *et al.* [27] measured the 168.8 GHz helium-broadened H_2S linewidth ($1_{0,1} - 1_{1,0}$) at 295K and report a value of 1.60 MHz/Torr (1.22 GHz/Bar). We assumed the same $\Delta\nu_{He}$ for the $2_{0,2} - 2_{1,1}$ transition.

The measured absorption in dB/m at 2 atm and 296K is shown in Fig. 4. The solid lines represent the theoretically computed absorption for several values of $\Delta\nu_{H_2}$. The line parameters used in the computation of H_2S absorption were taken from the GEISA line catalog [5], [8]. We used the Van Vleck-Weisskopf [24] lineshape with linewidth as given by (3). Visual inspection of Fig. 4 suggests a value of $\Delta\nu_{H_2}$ approximately equal to 2 ± 0.5 GHz/Bar (2.6 ± 0.7 MHz/Torr).

IV. Discussion

Fig. 5 shows the observed and computed emission from Jupiter near 217 GHz (1.4 mm). Our observed brightness temperatures (solid circles) and those of previous observations (open circles) are shown with corresponding error bars. The error bars include the statistical uncertainty (solid line) as well as the additional 10% uncertainty in the Martian flux (dashed line). The horizontal solid and dashed lines are synthetic spectra with and without H_2S opacity, respectively. The spectra were computed using the radiative transfer model described in [11].

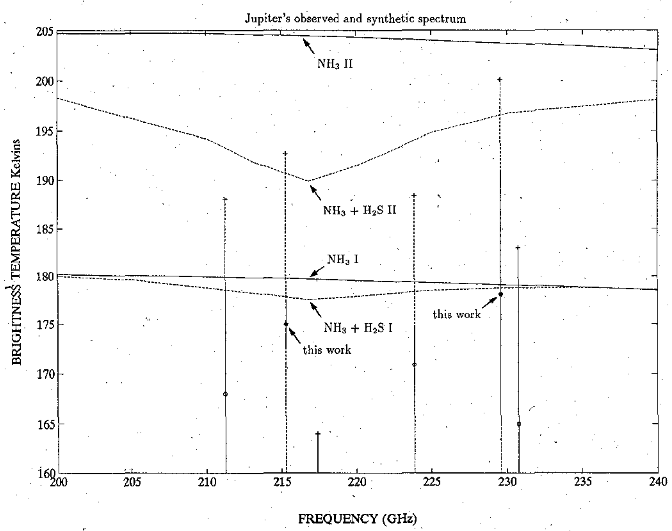

Fig. 5. Jupiter's observed and computed spectrum. •: our observations; ∘: previous observations. Error bars include the statistical uncertainty (solid line) and additional 10% uncertainty (dashed line) in the flux of Mars. Synthetic spectra with and without H_2S opacity (dashed lines and solid lines, respectively) using NH_3 and H_2S distributions in Fig. 6.

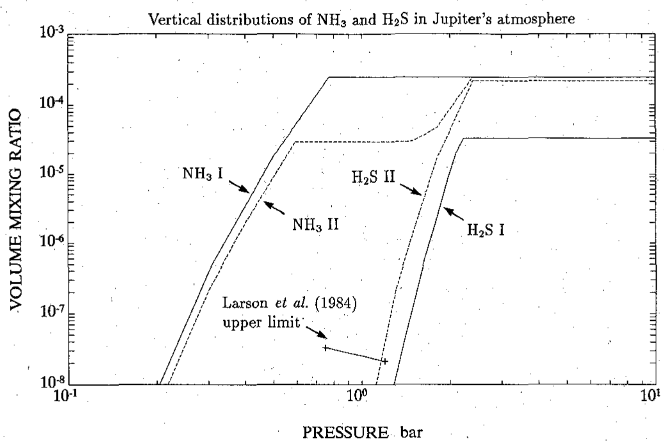

Fig. 6. NH_3 and H_2S vertical distributions based on thermo-chemical equilibrium models. H_2S upper limit from Larson *et al.* [13]. Deep mixing ratios: $\chi_{NH_3} = 2.5 \times 10^{-4}$; Model I: $\chi_{H_2S} = 3.35 \times 10^{-5}$ (solar); Model II: $\chi_{H_2S} = 2.2 \times 10^{-4}$.

We have computed Jupiter's emission by assuming two different vertical distributions of NH_3 and H_2S based on thermo-chemical equilibrium models. The mixing ratios as a function of pressure in Jupiter's atmosphere are shown in Fig. 6. We assumed a deep NH_3 mixing ratio equal to 2.5×10^{-4}. The deep NH_3 abundance is based on microwave and infrared observations [7], [4]. In case I (Fig. 6, solid lines), we assume a deep H_2S mixing ratio equal to 3.3×10^{-5}. This abundance is approximately equal to the solar H_2S abundance [1]. In case II (Fig. 6, dashed lines), we increased the H_2S mixing ratio to approximately 6 times the solar abundance (2×10^{-4}). In this case, NH_3 is significantly depleted in the 1–2 bar region by the reaction with H_2S to form solid NH_4SH.

Because we were unable to obtain repeatable observations at individual frequencies over several nights due to poor weather conditions, the uncertainties in our observed brightness temperatures were large. Therefore, we were unable to detect H_2S or set tighter limits on the H_2S mixing ratio in Jupiter's troposphere. However, we have obtained brightness temperatures of Jupiter (relative to Mars) near 1.4 mm at a higher spectral resolution than previously used.

V. Conclusions and Suggestions for Future Work

Although we were unable to obtain a positive H_2S detection or set tighter upper limits on the H_2S abundance in Jupiter's atmosphere, the search for H_2S at millimeter wavelengths should not be abandoned. Poor weather conditions and instrumental difficulties contributed to our large observational uncertainties. Given more ideal conditions, the statistical uncertainties could be significantly reduced and systematic effects eliminated. In order to further reduce the observational uncertainty, the integration time must be increased. Observations should be repeated over three or more nights. Weather conditions must also be exceptional in order to eliminate any variations in the observed brightness temperatures resulting from variations in the earth's atmospheric opacity. In addition, observations should be made at a minimum of three frequencies, corresponding to the H_2S line center and on both sides of the line near the continuum, in order to achieve a convincing detection of the H_2S line.

Improvements in millimeter-wave technology will make the detection of broad spectral features (i.e., pressure-broadened lines in planetary atmospheres) more feasible in the future. Wide-band oscillators coupled with computer-controlled tuning will significantly reduce the time required to tune receivers. New instruments, such as Fourier Transform Spectrometers with GHz resolution, will also be available for future use in planetary millimeter-wave spectroscopy.

Acknowledgment

We thank T. D. Groesbeck and A. Schinckel (CSO) for their generous help with the observation and data reduction at the CSO. The authors thank D. P. Champbell, J. J. Gallagher and S. Halpbern of the Georgia Tech Research Institute (GTRI) and T. E. Brewer (Georgia Tech) for their generous assistance with the laboratory equipment and for providing illuminating discussions in this area. We also thank D. J. Rudy (Jet Propulsion Laboratory) for providing us with Mars brightness temperatures from his model and E. Lellouch (Observatoire de Paris-Meudon) for helpful discussions.

References

[1] E. Anders and N. Grevesse, "Abundances of the elements: meteoritic and solar," *Geochim. Cosmochim. Acta*, vol. 53, pp. 197–214, 1989.

[2] S. K. Atreya and P. N. Romani, "Photochemistry and clouds of Jupiter, Saturn, and Uranus," in *Recent Advances in Planetary Meteorology*, G. E. Hunt, Ed. Cambridge, MA: Cambridge Univ. Press, pp. 17–68, 1985.

[3] B. Bezard, A. Marten, J. P. Baluteau, D. Gautier, J. M. Flaud, and C. Camy-Peyret, "On the detectability of H_2S in Jupiter," *Icarus*, 55, pp. 259–271, 1983.

[4] G. L. Bjoraker, H. P. Larson, and V. G. Kunde, "The gas composition of Jupiter derived from 5 μm airborne spectroscopic observations," *Icarus*, 66, pp. 579–609, 1986.

[5] A. Chedin, N. Husson, N. A. Scott, I. Cohen Hellalet, and A. Berroir, GEISA Data Bank, no. 3, 1982.

[6] R. Courtin, N. Coron, T. Encrenaz, R. Gispert, P. Bruston, J. Leblanc, G. Dambier, and A. Vidal-Madjar, "Observations of giant planets at 1.4 mm and consequences on the effective temperatures," *Astron. Astrophys.*, vol. 60, pp. 115–123, 1977.

[7] I. de Pater and S. T. Massie, "Models of the millimeter-centimeter spectra of the giant planets," *Icarus*, 62, pp. 143–171, 1985.

[8] J. M. Flaud, C. Camy-Peyret, and J. W. C. Johns, "The far infrared spectrum of hydrogen sulfide," *Can. J. Phys.*, vol. 61, pp. 1462–1473, 1983.

[9] M. J. Griffin, P. A. R. Ade, G. S. Orton, E. I. Robson, W. K. Gear, I. G. Nolt, and J. V. Radostitz, "Submillimeter and millimeter observations of Jupiter," *Icarus*, 65, pp. 244–256, 1986.

[10] P. Helminger and F. C. De Lucia, "Pressure broadening of hydrogen sulfide," *J. Quant. Radiat. Trans.*, vol. 17, pp. 751–754, 1977.

[11] J. Joiner and P. G. Steffes, "Modeling of Jupiter's millimeter-wave emission utilizing laboratory measurements of ammonia (NH_3) opacity," *JGR 96*, E2, pp. 17463–17470, 1991.

[12] E. Lellouch, F. Combes, and T. Encrenaz, "Microwave observations of Jupiter and Saturn," *Astron. Astrophys.*, vol. 140, pp. 216–219, 1984.

[13] H. P. Larson, D. S. Davis, R. Hofman, and G. L. Bjoraker, "The Jovian atmospheric window at 2.7 microns: A search for H_2S," *Icarus*, 60, pp. 621–639, 1984.

[14] G. F. Lindal, G. E. Wood, G. S. Levy, J. O. Anderson, D. N. Sweetnam, H. B. Hotz, B. J. Buckles, D. P. Holmes, P. E. Dams, V. R. Eshleman, G. L. Tyler, and T. A. Croft, "The atmosphere of Jupiter: An analysis of the Voyager radio occultation measurements," *J. Geophys. Res.*, vol. 86, pp. 8721–8727, 1981.

[15] D. O. Muhleman and G. L. Berge, "Observations of Mars, Uranus, Neptune, Io, Europa, Ganymede, and Callisto at a wavelength of 2.66 mm," *Icarus*, 92, pp. 263–272, 1991.

[16] T. G. Phillips, *Caltech Submillimeter Observatory (CSO) Handbook*, 1989.

[17] J. D. G. Rather, B. L. Ulich, and P. A. R. Ade, "Planetary brightness temperature measurements at 1.4-mm wavelength," *Icarus*, 23, pp. 448–453, 1974.

[18] D. J. Rudy, D. O. Muhlmenam, G. L. Berge, B. M. Jakosky, and P. R. Christensen, "Mars: VLA observations of the northern hemisphere and the northern polar region at wavelengths of 2 and 6 cm," *Icarus*, 71, pp. 159–177, 1987.

[19] D. J. Rudy, D. O. Muhlmenam, and G. L. Berge, "Mars: 2 cm and 6 cm VLA observations of the southern hemisphere and derived properties," *Icarus*, 1987.

[20] E. C. Sutton, G. A. Blake, C. R. Masson, and T. G. Phillips, "Molecular line survey of Orion from 215 to 247 GHz," *Astrophys. J. Supp. Ser.*, vol. 58, pp. 341–378, 1985.

[21] B. L. Ulich, J. H. Davis, P. J. Rhodes, and J. M. Hollis, "Absolute brightness temperature measurements at 3.5 mm wavelength," *IEEE Trans. Antennas Propagat.*, vol. AP-28, no. 3, pp. 367–377, 1980.

[22] B. L. Ulich, "Millimeter-wavelength continuum calibration sources," *Astron. J.*, 86, pp. 1619–1626, 1981.

[23] B. L. Ulich, J. R. Dickel, and I. dePater, "Planetary Observations at a wavelength of 1.32 mm," *Icarus*, 60, pp. 590–598, 1984.

[24] J. H. Van Vleck and V. F. Weisskopf, "On the shape of collision-broadened lines," *Rev. Mod. Phys.*, vol. 17, pp. 433–443, 1945.

[25] J. W. Waters, "Absorption and emission of microwave radiation by atmospheric gases," in *Methods of Experimental Physics*, M. L. Meeks, Ed., Pt. B, Radio Astronomy, New York: Academic Press, Sect. 2.3, 1976.

[26] R. A. West, D. F. Strobel, and M. G. Tomasko, "Clouds, aerosols, and photochemistry in the Jovian atmosphere," *Icarus*, 65, pp. 161–217, 1986.

[27] D. R. Willey, T. M. Goyette, W. L. Ebenstein, D. N. Bittner, and F. C. DeLucia, "Collisionally cooled spectroscopy: Pressure broadening below 5K," *J. Chem. Phys.*, vol. 91, pp. 122–125, 1989.

Joanna Joiner (S'91–M'91) received the S.B.(E.E.), S.M.(E.E.), and Ph.D.(E.E.) degrees from the Georgia Institute of Technology in 1987, 1988, and 1991, respectively.

She was employed by Consultant's Choice, Inc., from 1985 to 1987, where she was involved in the design and implementation of a power-line MODEM. Her doctoral research concentrated on the millimeter-wave spectra of the Jovian planets. This research included laboratory measurements of the millimeter-wave opacity of gases under simulated planetary conditions, modeling of the emission from the Jovian planets, and radio astronomical observations of Jupiter. Dr. Joiner is currently employed by the Universities Space Research Association at NASA/Goddard Space Flight Center. She is currently involved in satellite remote sensing of the terrestrial atmosphere using the AIRS/AMSU instrument (an infrared and microwave radiometer selected to fly on the EOS-A series satellites). Her current research involves simulating AIRS/AMSU retrievals of surface parameters as well as temperature, water vapor, and ozone profiles under clear and cloudy conditions.

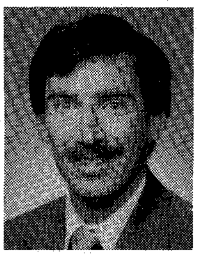

Paul G. Steffes (S'82–M'83–SM'89) received the S.B.(E.E.) and S.M.(E.E.) degrees from MIT in 1977, and the Ph.D.(E.E.) degree from Stanford University in 1982. At MIT, he was involved in the development of a 118 GHz radiometer system to measure atmospheric absorption by oxygen at the 2.5 millimeter wavelength. From 1977 to 1982, Dr. Steffes worked at Watkins-Johnson in the design and development of millimeter-wave receiving systems. His doctoral research concentrated on microwave radio occultation experiments using the Voyager and Mariner spacecraft, with specific interest in microwave absorption in planetary atmospheres.

He joined the faculty at the Georgia Institute of Technology in 1982, and is currently an Associate Professor of Electrical Engineering. Research at Georgia Tech has included design of microwave systems for remote sensing, study of the microwave and millimeter-wave properties of planetary atmospheres, radio astronomy, and satellite communications systems. His current research interests include microwave and millimeter-wave remote sensing of planetary atmospheres (including Earth's), microwave and millimeter-wave communications satellite systems, radio and radar astronomy systems and techniques, non-invasive monitoring of glucose levels in the human body, and electromagnetic theory. Dr. Steffes is involved with several space missions including Pioneer-Venus, Magellan, and the NASA-SETI (Search for Extra-Terrestrial Intelligence) Microwave Observing Project.

Keith S. Noll received the Ph.D. in astronomy from the State University of New York at Stony Brook in 1987.

His research has focused on the problem of determining elemental and molecular abundances of astronomical objects from infrared spectra. He has discovered several new compounds in the atmospheres of Saturn and Jupiter including AsH_3, GeH_4, and CO. He extended his work as a postdoctoral research associate at the University of Arizona's Lunar and Planetary Laboratory from 1987 to 1990. He participated in several missions on NASA's Kuiper Airborne Observatory aimed at solar system and interstellar medium targets. From 1990 to 1991 he held a National Research Council Fellowship at NASA's Marshall Space Flight Center where he was involved in long range planning for orbital and lunar-based telescopes. He also began a long term observing campaign to monitor changes in Saturn's moon Titan to provide an observational baseline for NASA's planned Cassini/Huygens mission. Dr. Noll is now an Assistant Astronomer at the Space Telescope Science Institute in Baltimore where he coordinates long-range planning for observation of solar system targets by the Hubble Space Telescope as well as continuing his research into the chemical composition of the planets.